

Monitoring of zincate pre-treatment of aluminium prior to electroless nickel plating

S. Court,² C. Kerr,^{2,+} C. Ponce de León,¹ J.R. Smith,² B.D. Barker,² F.C. Walsh*¹

¹ Electrochemical Engineering Laboratory & Materials Engineering Group, Engineering Sciences, University of Southampton, Highfield, Southampton, SO17 1BJ, UK.

² School of Pharmacy and Biomedical Sciences, University of Portsmouth, St Michael's Building, White Swan Road, Portsmouth PO1 2DT, UK.

+ Current address: Atotech (China) Chemicals Ltd, Shanghai Qingpu Branch No. 5399, Plant A6, Wai Qing Song Road, Qingpu District, Shanghai, China 201707.

*Author for correspondence.

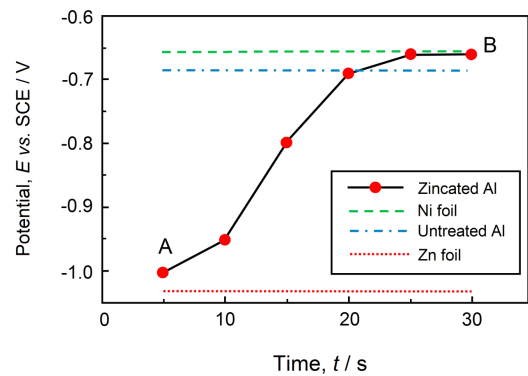
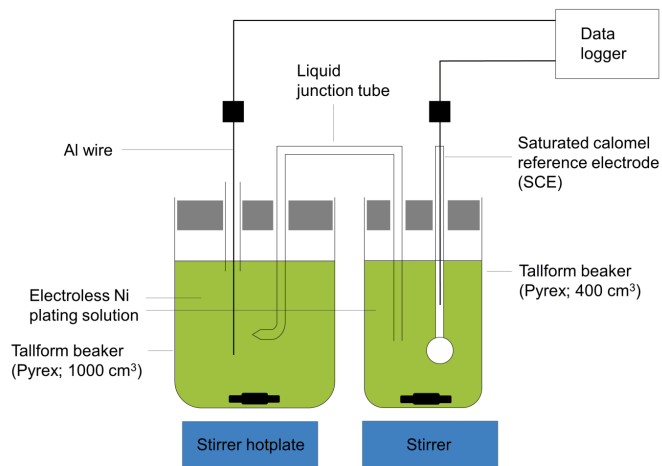
Abstract

Zincating is used as a pre-treatment for aluminium prior to electroless nickel deposition during preparation of magnetic computer memory discs. Four immersion zincating solutions were evaluated at 22 °C using single step or double zincating followed by electroless nickel deposition from a high phosphorus hypophosphite bath at 90 °C. The coating process was monitored by potential vs. time curves obtained under open-circuit conditions during zincating then electroless nickel plating. The surface morphology of the aluminium, at various stages, was imaged by scanning electron microscopy and atomic force microscopy. Zero resistance ammetry was used to record galvanic currents between the aluminium and an inert platinum counter electrode during zincating. This together with potential-time measurements provided simple and valuable methods for following the zincating process and subsequent electroless Ni plating. Double zincating enabled a shorter induction time for electroless Ni deposition and resulted in a more complete coverage of the surface by Zn.

Keywords: Electrode potential; electroless nickel; immersion plating; process monitoring.

Highlights

- Zincating of aluminium is monitored by open-circuit potential measurements.
- Potentiometric monitoring is complemented by SEM and AFM imaging.
- Double zincating results in superior electroless nickel deposits.
- Four zincating immersion pretreatments are compared.
- Proprietary zincating showed faster zinc nucleation and growth and a more complete film.



1. Introduction

The process of coating aluminium with electroless nickel can be achieved if the Al provides a catalytic substrate.¹ Al is very reactive and typically forms a *ca.* 0.02 μm thick surface oxide film when exposed to the atmosphere. The oxide is detrimental to Ni coatings as it prevents metallic bonding between the coating and the substrate, leading to poor adhesion, blistering and coating failure.

Zincating can be successfully used to remove the oxide, cover the Al with a thin layer of Zn and prevent the oxide from reforming. When immersed in electroless Ni solution, the Zn layer will dissolve and codeposit with electroless Ni at the interface between substrate and coating.²⁻⁶

Zincate baths are usually alkaline solutions of zinc oxide. Modified alloy zincate pre-treatments⁷ contain metallic additives such as Ni, Cu and Fe. This produces a thinner, more compact alloy layer that enhances adhesion by developing a finer grained, thinner deposit.^{7,8} Al alloys contain metallic constituents which are unreactive during the displacement reaction. The metallic additives control the thickness of the immersion layer by inhibiting the displacement reaction occurring at the Al surface.⁹ This leads to a more uniform and continuous, thinner deposit. Ritchie *et al.*¹⁰ describe the addition of iron (III) chloride complexed with potassium sodium tartrate. The tartrate alone was shown to have no effect on the zincate process, although the presence as a complexing agent kept Fe^{3+} in solution. The FeCl_3 was found to reduce the size of the Zn crystals as they formed, producing a more crystalline coating.

Alkaline cleaners are used to remove soils or dirt that may have been left during the manufacturing of the Al component. Alkaline cleaners may contain silicates that prevent the Al from being etched, borates to provide buffering and phosphates to remove grease and oils.¹¹ There are environmental concerns over borate and silicate cleaners, which have the potential to produce insoluble metallic silicates and this has led to the development of borate- and silicate-free alkaline cleaners. A water rinse is necessary after the after all steps to prevent any drag-in and to prevent any cross-contamination between pre-treatment chemicals.

An acid etch, which usually contains mixtures of sulphuric and phosphoric acids, is the first step in removing the oxide film. The Al is immersed in acid before it is transferred to the desmut cleaning solution which usually contains nitric acid (50% vol. HNO₃) but can also contain sulphuric acid and fluoride compounds.⁹ The desmut procedure is intended to remove non-adherent reaction products (such as oxides of Si, Mg, *etc.*) which remain after etching. A simple immersion deposit of Zn can then replace the oxide film on the Al. The Zn layer is usually achieved by immersing the Al substrate in an alkaline zincate solution, the overall process being represented by (1) and (2):^{12,13}

Dissolution of the Al substrate:



is accompanied by the deposition of Zn from an alkaline, zincate ion containing solution according to:



together with the evolution of H₂:



A double zincating step involves stripping the initial zincate layer in HNO₃ (50% vol.) then re-zincating, is used to give a thinner, more uniform coating.¹⁴ The addition of additives such as hydrofluoric acid (2% vol.), in the nitric acid strip, has been shown to improve this process.⁷

Dissolution of the Zn film occurs when the zincated Al is immersed into the electroless Ni plating bath and is co-deposited with the Ni. A Zn-rich zone is then found to exist between the electroless Ni deposit and the Al substrate. This Zn-rich zone can often lead to adhesive and cohesive failure.^{3,5} Adhesive failures are found in deposits from electroless Ni baths having high deposition rates and short induction times. Cohesive failures occur when deposition conditions lead to the formation of narrow Zn-rich zones of relatively high Zn content. The adhesion of electroless Ni to the zincated Al is dependent on the composition of the zincating solution, the composition of the Al alloy, the electroless Ni bath itself^{13,15} and the process conditions.

Zincating is a long-standing and widely accepted pretreatment for Al alloys prior to electroless deposition or electroplating of Ni. An example is the Bondal™ process, introduced by Canning Materials (later Macdermid) Ltd. And the process was enhanced in the 1980s by double immersion zincating.^{16,17} Despite the success of such processes, there has been a continuing need for improved control of zincate film porosity, continuity and completion.

The present studies were motivated by the need to characterise zincating prior to electroless Ni plating of Al discs for typical use as memory storage media for personal computers. Extensive use of open-circuit potential measurements¹⁸ was made due to their simplicity, low cost and simple instrumentation. Such potentiometric methods have proved to be an elegant means of determining defects in plated metallic coatings, *e.g.*, through porosity of electrodeposited metal coatings,¹⁹ the monitoring of phosphating of steel²⁰, electroless Ni coatings on steel²¹ and corrosion of metals at open-circuit.²² Surface morphology has also been investigated by SEM and atomic force microscopy (AFM).^{23,24} Preliminary studies have been summarised in a previous paper.²⁵

2. Experimental procedure

2.1 The induction time for electroless Ni deposition

Pure AnalaR Al wire was subjected to a single and double zincating immersion which varied from 0 to 120 s. Where a double step was used, the first zincating immersion time was fixed at 60 s. The complete pre-treatment stages and material composition are discussed in detail in sections 2.3 and 3.1. Four different zincate solutions were used: Fidelity 3116M (at 20% and 40% concentration) and two synthetic zincate solutions ('dilute' and 'concentrated') comprising ZnO (AR grade; 15 g dm⁻³) and NaOH (AR grade; 100 g dm⁻³) for the dilute samples and ZnO (70 g dm⁻³) and NaOH (450 g dm⁻³), for the concentrated solution. In line with industrial practice, the zincate solutions were maintained near room temperature (22 °C) while the electroless plating baths were used at a temperature of 90 °C to provide relatively high deposition rates. Two commercial, high phosphorus electroless Ni baths were used at a temperature of 90 °C to achieve a relatively high deposition rate: Fidelity 4355 and 5010. The latter was developed to improve deposit thermomagnetic stability and to have a higher corrosion resistance than deposits from the Fidelity 4355 solution.

An Al wire was immersed into the electroless Ni baths with the potential monitored with respect to a standard calomel reference electrode (SCE; Fig. 1). A datalogger (an Extech 383274 high impedance digital multimeter) was used to monitor the potential of the zincated Al in the electroless Ni bath and the induction of plating was calculated from the point where the curve began to level out. For the commercial zincating bath, the plating potential was at *ca.* -670 mV *vs.* SCE for the Fidelity 5010 solution and -640 mV *vs.* SCE for the Fidelity 4355 solution.

2.2 Galvanic current measurements

The galvanic current over time was monitored as the current recorded on a ZRA between the sample being coated and a Pt mesh counter electrode (3 cm^2). The readings from the ZRA instrument were recorded with a datalogger in a similar manner to the potential-time curves.

2.3 Zn deposition

The weight gain analysis for assessment of the thickness of the zincate coating was calculated using strips of commercially pure Al (grade 3105 H24). This material contained 0.60% Si, 0.70% Fe, 0.30% Cu, 0.30–0.80% Mn, 0.20–0.80% Mg, 0.20% Cr and 0.40% wt. Zn, the remainder being Al.

The time of immersion in the zincating solution was varied from 0 to 120 s. The samples were then washed in alcohol, dried in a hot air stream and weighed. The zincate layer was chemically stripped off the Al surface using HNO_3 (50% vol.; AnalaR), water rinsed, dried and reweighed. The coating mass was then calculated. A second zincating stage was undertaken (with the first step fixed at 60 s) and the mass of Zn deposited was calculated in a similar manner.

2.4 Surface morphology

To show the nature of the deposit, Al which had been coated with a single and double zincate deposit was examined using scanning electron microscopy (SEM; JOEL JSM-6100) and atomic force microscopy (AFM; Discoverer TMX2000 Scanning Probe Microscope, ThermoMicroscopes, CA, USA). Samples were mounted on Al stubs and magnetic Ni discs for SEM and AFM studies, respectively, using carbon-loaded, double-sided adhesive tape. For the latter technique, contact mode, in air, was used and V-shaped, silicon nitride probes (spring constant, $k = 0.032 \text{ N m}^{-1}$), bearing standard profile tips, were employed. AFM was performed using a $70 \times 70 \times 12 \text{ }\mu\text{m}^3$ tripod scanner. AFM images were rendered in a pseudo-3D format and grain diameters ($N = 10$), surface roughness (arithmetic roughness average, R_a and root-mean-square roughness, R_{RMS} both using a projected area of $100 \text{ }\mu\text{m}^2$) measurements^{26,27} and surface area (actual surface area / projected area ($100 \text{ }\mu\text{m}^2$)) measurements were obtained using WSxM Solutions freeware software (Version 4.0 Beta 8.1; Madrid, Spain).²⁸

3. Results and discussion

3.1 Induction of electroless Ni deposition

A convenient method to study the nature of the surface during electroless plating of Al was by monitoring the electrode potential of the metal surface. Before electroless Ni could be plated on to the Al surface, the Zn dissolved and the potential of the sample became less negative (Fig. 2). Point A represents the potential at which the zincate layer began to form (*ca.* -1.00 V vs. SCE). At point B, the potential levelled out at -0.66 V vs. SCE as the surface was covered with a continuous deposit of electroless Ni. The time required for the complete dissolution of the zincate layer could then be estimated.

The expected potential of uncoated Al was -0.685 V vs. SCE. A Zn covered Al surface had a value of -1.03 V vs. SCE while a perfect coating of electroless Ni on Al had a value of *ca.* -0.66 V vs. SCE. By following the variation of potential with time, the change in the nature of the surface during the early stages of electroless deposition could be tracked.

Typical potential vs. time plots for single and double zincating procedures are shown in Fig. 3. The pre-treatment procedure was kept constant so that a direct comparison could be made. The induction times of electroless Ni deposition for a single zincate pre-treated surface in the Fidelity 4355 bath varied from 22 to 27 s on increasing the zincating time from 15 to 120 s in an aqueous 40% Fidelity 3116M zincating solution (Table 1). When the concentration of the zincating solution was reduced to 20% vol., the time taken for the induction of electroless Ni increased from 28 to 36 s. In the Fidelity 5010 bath, the induction time for electroless Ni deposition increased from 23 to 48 s in a 20% vol. zincating solution and 32 to 45 s for a 40% vol. zincating solution.

In general, the induction of electroless Ni plating increased as the concentration of the zincating bath was reduced. Zelle reported an increase in the thickness of zincate deposits with less concentrated baths.²⁹ Robertson *et al.* also reported this and suggested that at stronger concentrations, the whole of the Al surface is covered with a thin layer of Zn that blocks any further reaction.³⁰ At lower concentrations, incomplete coverage leads to further dissolution of Al and a thicker coating as more of the anodic substrate sites are exposed to the solution.

For the double zincating pre-treatment, the first zincating step was fixed at 60 s and the time of the second zincate was varied from 15 to 120 s. When using the Fidelity 4355 solution, the induction of electroless Ni increased from 18 to 29 s for a 40% solution and from 16 to 23 s for a 20% solution.

The commercially available zincating solutions were tested at the maximum (40% vol.) and minimum (20%) recommended strength. In a 20% vol. solution, the time for the dissolution of Zn increased with increasing zincating and showed the gradual build-up of Zn on the Al wire. For a double zincating procedure, altering the concentration of the zincate solution led to similar induction times of electroless Ni, indicating that the concentration of zincating solution was not that critical for the efficiency of a double zincate treatment of this substrate.

For the concentrated zincate solution, followed by electroless Ni deposition in a Fidelity 5010 bath, the induction times increased from 14.4 to 19.2 s after immersion in the zincate solution for 1 min. Overlapping of the curves in Figure 3d) suggested that the maximum thickness of Zn had been reached. This was not so apparent for the equivalent procedure in the Fidelity 4355 bath, which showed slightly higher induction times (Table 1).

When the double zincating procedure was employed, the times for the induction of electroless Ni in both plating solutions were similar, ranging from 10 to 15 s as the double zincating immersion was increased. After 1 minute immersion, the curves converge, again indicating that the maximum thickness of Zn had been reached on the Al substrate.

In the case of the diluted zincate solution, the induction of electroless Ni in Fidelity 5010 was slightly higher than the concentrated solution and ranged from *ca.* 14 to 28 s. The same trend was also seen in the commercially available baths. The double procedure also gave slightly higher induction times from 13.6 to 18.4 s. In the Fidelity 4355 bath, both procedures gave slightly lower induction times, possibly

due to the differences in plating potential. The Fidelity 4355 bath allowed deposition at a slightly lower potential and the time taken to reach this potential was slightly lower.

The increase in starting potential as the Al was placed in the electroless Ni bath when a double zincating method was used can be explained by a more complete coverage of the surface. The SEM micrographs also showed a much smoother surface when a double zincating procedure was employed. For the laboratory prepared solutions, this increase in starting potential was not well defined, indicating a rougher, less completely covered surface. The main differences between the zincating solution is the presence of additives such as Fe^{3+} and tartrate, which would account for the differences in the shape of the curves between the commercial and laboratory prepared solutions.

There are also differences in the plating potential between the electroless Ni baths and the commercial and laboratory prepared zincate solutions. There were no significant differences between a single and double zincating procedure. There was a difference, however, between the Fidelity 4355 and 5010 plating solutions. Fidelity 5010 was developed to give an improved corrosion resistance to that of 4355 so differences in the bath 'make up' are expected to produce differences in the potential. The differences were also apparent when monitoring the galvanic current over time in Fig. 4a with the Fidelity 5010 bath showing a lower current flowing than in the 4355 bath, *i.e.*, fewer active Al sites were exposed to the electrolyte to sustain a galvanic current at open-circuit.

To assess the nature of electroless Ni depositing on Al over longer periods, potential *vs.* time curves were monitored over 1 hour. These are shown in Fig. 4b and confirm the deposition potential of the process over a longer time period. The open-circuit galvanic current was also monitored over the same period.

3.2 Calculation of zincate layer thickness

The variation in deposit thickness for single and double zincating steps using a 20% and 40% Fidelity 3116M zincate solution are shown in Figs. 5a and b. At 20% vol., the thickness of a single zincate deposit increased from 5 to 9 μm whilst the thickness of a double zincate deposit typically levelled out at around 4-5 μm . The thickness of a single zincating step increased from 8 to 16 μm . The thickness of the deposit using a double zincate was also lower than a single zincating step, increased from 4 to 7 μm . Using a commercial zincating bath, the double zincate had a thinner coating than the single zincate and increasing the concentration increased the thickness for a single step, whereas concentration had little effect on the double zincating step.

Deposit thickness variations from the laboratory prepared dilute zincate solution are shown Fig. 5. The thickness of a single zincate increased from 6 to 9 μm , whereas the thickness of the double zincate which was significantly reduced, increased from 1 to 5 μm . For the laboratory prepared concentrated zincate solution, the thickness of the single zincate remained similar at *ca.* 10 μm , whereas that of double zincate remained constant at *ca.* 3 μm . Using a laboratory prepared zincating bath, the resulting double zincate had a thinner coating than the single zincate and increasing the concentration produced similar thicknesses for a single and double zincating step.

Laugton³ reported that the thickness of zincate coating increased from 1.6 μm to 22 μm after three minutes immersion time on increasing the temperature from 16 to 32 $^{\circ}\text{C}$. It is unclear whether these values are based on a single or double zincating step although the authors demonstrated that the thickness of the zincate layer increased with temperature.

The thickness of Zn deposited onto the Al can also be seen to affect the induction of electroless Ni plating times as the first zincating step typically had a greater dissolution time than the equivalent time of the second zincating step. Altering the zincating concentration resulted in small differences in the calculated Zn thickness.

3.3 Microscopy

The single zincating step of 60 s in Fidelity 3116M, with a typical thickness of 12 μm , showed complete coverage of the Al surface, which followed closely the contours of the substrate (Fig. 6a). The rolling lines were clearly visible and at higher magnification, minute Zn grains were apparent. The double zincating step produced a smoother surface with the absence of rolling lines due to the etching of the surface during the stripping cycle (Fig. 6b). Pits were also seen that may be due to etching of the Al during the removal of the first zincate layer. This could be caused by dissolution of intermetallic phases or occluded particles from the cold working of the Al sheet.

AFM images of the Al surface after single and double zincate treatments revealed granular-like deposits (Fig. 7). The grains were larger in the single zincate treated surface than those on the double zincate surface (*dia.*: 446 ± 114 and 209 ± 39 nm, respectively). This was also reflected in the surface roughness measurements (single and double zincate: $R_a = 52.1$ and 32.0 nm, $R_{RMS} = 76.0$ and 42.4 nm, both respectively) and surface area measurements (the ratio of actual surface area to projected area ($100 \mu\text{m}^2$) for single and double zincate: 1.10 and 1.08). Defects were also more prevalent on the single zincate treated surface in Fig. 7a) and b) than on the double treated surface. Both SEM and

AFM imaging techniques were therefore valuable in accessing the topography of the surface following zincating treatments.

Monteiro *et al.*⁶ studied the effects of concentration and temperature of NaOH, HNO₃ and HF pre-treatment solutions on the morphology of Al surfaces. SEM imaging and EDS analysis indicated that NaOH solutions produced etch pits but failed to etch FeAl₃ particles. Acid treatment preferentially removed these particles, without altering the surface roughness. In an attempt to improve the coverage rate of Zn alloy films, which were chemically deposited prior to Ni electroplating, a pre-treatment sequence of double-step immersion in HNO₃ and HF solution, with NaOH treatment between the two acid steps was used. The results showed that the first acid step removed most of the large FeAl₃ particles, as well as the previous oxide layer, while the alkaline treatment generated surface micro-roughness on the surface to produce shallow cellular cavities in a honeycomb structure. The acid treatment preferentially etched smaller FeAl₃ particles and the most prominent surface heterogeneities. Such a pre-treatment sequence was considered more effective than previous ones and produced a clean, catalytic surface to promote nucleation and growth of Zn films. The adhesion of Ni electrodeposits to the surface was tenfold higher than those for conventional two-stage processes. The authors considered that their results were due to improved surface homogeneity due to the removal of second-phase particles and the small and uniform dimensions of the cells produced by the etch treatment, resulting in good surface coverage.

Khan *et al.*^{31,32} confirmed earlier findings by Szasz *et al.*³³ and Martyak,³⁴ where the surface characterisation of the zincated Al and selected alloys was studied using SEM in the early stages of autocatalytic, electroless Ni deposition.

Murakami *et al.*³⁵ considered the detailed morphology and structure of zincate films formed as a pre-treatment for electroless Ni-phosphorus coatings on commercial pure Al. By using a simple solution of NaOH and ZnO, a zincate film formed by single zincate treatment showed coarse Zn grains as large as 1–2 μm in size whose (0001) planes were mainly parallel to the surface of the substrate. A double zincate treatment using the basic solution reduced the coarse grains, and the thickness of the uniform zincate film was 30–40 nm. A commercial zincate solution, which contained Fe, decreased the number and size of coarse Zn grains for the single zincate treatment compared to that from the basic solution, and the double zincate treatment formed a further thin zincate film thickness of 10–20 nm. The single zincate treatment by using the basic zincate solution resulted in such poor adhesive strength of the electroless Ni-phosphorus plated film as to peel off the substrate due to its residual stress. Measurement of adhesive strength by a peeling test showed the double zincate pre-treatment increased the adhesion of the plated film up to 30 N m^{-1} . In the case of the commercial zincate solution, the adhesive strength obtained by the single zincate treatment was 125 N m^{-1} . The adhesion of the plated Ni-phosphorus film was too strong to conduct a peeling test in the case of double zincate treatment in a commercial solution and ductile fracture of the substrate was seen. Gaps were identified at the interface between the Ni-phosphorus plated film and the substrate by TEM imaging in the case of the double zincate treatment by the basic zincate solution. However, such gaps were removed and strong adhesion was obtained after double zincate treatment by the commercial solution.

The effect of zincate film formation on the adhesion of electroless Ni-phosphorus plated films on binary Al alloys of Al-2% at. Mn, Al-2% at. Fe, Al-2% at. Cu, Al-2% at. Zn and high-purity Al (99.999% wt.) was studied recently by Murakami *et al.*³⁶ Zn deposition during zincate immersion was dependent on alloying elements present in the substrate. For the first and second zincate treatments of

Al-Mn, Al-Fe and high-purity Al, Zn excessively precipitated, resulting in porous, easily removed films of Zn. The surfaces of the Al-Cu and Al-Zn alloys were immediately coated by uniform zincate films during first and the second zincate immersions. The authors considered the precipitation of Zn to be uniform if the oxide film on the substrate uniformly and rapidly dissolved in the zincate solution. When electroless Ni-phosphorus deposition took place after the second zincate immersion of the Al-Mn and Al-Fe alloys, the plated films readily peeled off, in contrast to excellent adhesion on Al-Cu and Al-Zn alloys. Poor adhesion was attributed to dissolution of excess Zn at the beginning of the plating, the hydrogen gas generated resulting in voids between plated film and substrate.

3.4 General considerations

The studies in this paper were intended to examine a simple, readily available electrochemical measurement to be used in the screening of zincating solutions and pre-treatment stages. The electrode potential decay curve over the first few seconds of plating, using a commercial zincating process (Fidelity 3116M) and laboratory prepared solutions. This provided an indication of the thickness of Zn deposited on to the surface of the Al substrate and the rate of induction of electroless Ni from the bath. The thickness of the zincate deposit was examined with time of immersion in the zincate bath using weight gain analysis, and the surface morphology was studied using SEM and AFM.

Fig. 8 shows schematic cross-sections of the surface layers on an Al alloy substrate following various zincate pre-treatments: (a) single zincate in synthetic laboratory solution, (b) double zincate in synthetic laboratory solution, (c) single zincate in proprietary solution, and (d) double zincate in a proprietary solution. Double zincating provided consistently shorter induction times for Zn nucleation while the commercial zincating solutions gave more complete, dense Zn coatings at a given time.

This research formed part of a programme to study electroless Ni deposition of on Al substrates for use in the computer memory disk industry. Memory disks consist of an Al alloy substrate subsequently is coated with electroless Ni then covered by a thin film magnetic coating followed by a protective carbon coating. The demand for increased storage space on computer memory disks is dependent on reducing the defects found in the layers below the magnetic memory film⁷. Therefore, the reduction in surface defects incorporated in the electroless Ni layer such as pores, nodules and magnetisation will greatly increase the performance of these disks. Electroless Ni is used as a protective coating for the Al alloy substrate to prevent pitting during the sputtering process used to deposit the magnetic recording layer. A variety of complementary DC electrochemical techniques have been used to follow corrosion and porosity in thin electrodeposited layers, open-circuit electrode potential vs. time measurements being the simplest, needing only a reference electrode and a high impedance DVM.³⁷

The corrosion resistance of electroless Ni deposits has been shown dependent on the surface roughness of the substrate,⁸ pre-treatment procedure⁹ and bath age¹⁰ as well as the composition and structure of the coating.¹ The overall aim of this paper was to study the pre-treatment procedure and the effect of additives on the deposition together with an assessment of corrosion resistance of electroless Ni on Al alloy substrates. This was achieved by the development of an electrochemical process to be used in the screening of various zincating solutions and pre-treatment procedures.

Achieving zincate film completion and continuity is important in the pretreatment of Al alloys prior to electroless Ni deposition and open-circuit electrode potential measurement can contribute a useful means of monitoring the efficiency of pretreatment.

The use of traditional, mixed potential theory to study the effects of additives on the electroless Ni plating process, deployment of known electrochemical techniques were also used to evaluate the effects of additives on the corrosion resistance of electroless Ni deposits and to distinguish between similar high phosphorus deposits will be considered in a separate paper.³⁸

4. Conclusions

1. The zincating of Al surfaces as a pre-treatment prior to electroless Ni deposition has been studied by techniques including open-circuit electrode potential *vs.* time and coating thickness *vs.* time. The resulting surfaces were imaged using SEM and AFM.
2. Potential-time measurements provided a simple and valuable method to monitor zincating followed by electroless Ni plating.
3. Double zincating enabled a shorter induction time for electroless Ni deposition and resulted in a more complete coverage of the surface by Zn.
4. Electrode potential monitoring can be used to follow the deposition process *in situ*. A double zincate treatment promoted early and facile nucleation and growth of complete electroless Ni layers.

Acknowledgements

The authors are grateful to OMI Fidelity for financial support.

References

1. W. Riedel, *Electroless Nickel Plating*. Finishing Publications Ltd, Stevenage, UK, 1991.
2. R.G. King, *Surface Treatment and Finishing of Aluminium*, Pergamon Press, Oxford, 1988.
3. R.W. Laughton: *Trans. IMF*, 1992, **70**, (3), 120–122.
4. K.P. Thurlow: *Trans. IMF*, 1989, **67**, (3), 82–86.

5. F.J. Monteiro, M.A. Barbosa, D.R. Gabe, D.H. Ross: *Plating Surf. Finish.*, 1989, **76**, (6), 86–89.
6. F.J. Monteiro, M.A. Barbosa, D.R. Gabe, D.H. Ross: *Surf. Coat. Technol.*, 1988, **35**, (3-4), 321–331.
7. T. Pearson, S.J. Wake: *Trans. IMF*, 1997, **75**, (3), 93–97.
8. F.J. Monteiro, M.A. Barbosa, D.H. Ross, D.R. Gabe: *Surf. Interface Anal.*, 1991, **17**, (7), 519–528.
9. M. Zitco, P. Vignati: Advances in electroless nickel and post treatment for enhanced corrosion protection of aluminium connectors. *Proc. 80th AESF Annual Technical Conference*, 1993, 1001–1011.
10. S. G. Robertson, I. M. Ritchie: *J. Appl. Electrochem.*, 1997, **27**, (7), 799–804.
11. D. Crotty, B. Clark, J. Greene, B. Durkin: *Plating Surf. Finish.*, 1992, **79**, (2), 42–48.
12. N. Wernick, R. Pinner, P.G. Sheasby: *The Surface Treatment and Finishing of Aluminium and its Alloys*, 5th Edn., Finishing Publications Ltd. Teddington, Middlesex, England, 1987, Volume 2.
13. G.O. Mallory: *Plating Surf. Finish*, 1985, **72**, (6), 86–95.
14. I.M. Sukonnik, J.S. Judge, W.T. Evans: *J. Miner. Met. Mater. Soc.*, 1989, 41, (8), 37–39.
15. M. Paramasivam, G. Suresh, B. Muthuramalingam, S. V. Iyer, V. Kapali: *J. Appl. Electrochem.*, 1991, **21**, (5), 452–456.
16. A.E. Wyszynski: *Trans. IMF*, 1967, **45**, 147–154.
17. A.E. Wyszynski: *Trans. IMF*, 1980, **58**, 34–40.
18. G.A. Ottewill, F.C. Walsh: *Trans. IMF*, 1992, **70**, (3), 141–143.
19. C. Kerr, B.D. Barker, F.C. Walsh: *Trans. IMF*, 1997, **75**, (2), 81–87.
20. B.D. Barker, P. Bond, P. Graham, T. Hoy, A.H. Nahlé, G.A. Ottewill, F.C. Walsh: *Arabian J. Sci. Eng.*, 1995, **20**, (2), 343–359.
21. C. Gabrielli, F. Raulin: *J. Appl. Electrochem.*, 1971, **1**, 167–177.
22. G. Kear, B.D. Barker, F.C. Walsh: *Corr. Sci.*, 2004, **46**, (1), 109–135.

23. J.R. Smith, S. Breakspear, S.A. Campbell: *Trans. IMF*, 2003, **81**, (2), B26–B29.
24. P. Eaton, P. West: *Atomic Force Microscopy*, Oxford University Press, 2010.
25. S.W. Court, B.D. Barker, F.C. Walsh: *Trans IMF*, 2000, **78**, (4), 157–162.
26. J.R. Smith, S. Breakspear, S.A. Campbell: *Trans. IMF*, 2003, **81**, (3), B55–B58.
27. L. Anicai, S. Costovici, A. Cojocar, A. Manea, T. Visan: *Trans. IMF*, 2015, **93**, (6), 302–312.
28. I. Horcas, R. Fernández, J.M. Gómez-Rodríguez, J. Colchero, J. Gómez-Herrero, A.M. Baro: *Rev. Sci. Instrum.*, 2007, **78**, (1), 013705.
29. W.G. Zelle: *J. Electrochem. Soc.*, 1953, **100**, (7), 328–333.
30. S.G. Robertson, I.M. Ritchie, D.M. Druskovich: *J. Appl. Electrochem.*, 1995, **25**, (7), 659–666.
31. E. Khan, C.F. Oduoza, T. Pearson: *J. Appl. Electrochem.*, 2007, **37**, (11), 1375–1381.
32. E. Khan, C.F. Oduoza: *J. Mater. Sci. Eng. A*, 2011, **1**, 457–471.
33. A. Szasz, J. Kojnok, L. Kertesz, Z. Paal, Z. Hegedus: *Thin Solid Films*, 1984, **116**, (1-3), 279–286.
34. N.M. Martyak: *Chem. Mater.*, 1994, **6**, (10), 1667–1674.
35. K. Murakami, M. Hino, M. Hiramatsu, K. Osamura, T. Kanadani: *Mater. Trans.*, 2006, **47**, (10), 2518–2523.
36. K. Murakami, M. Hino, M. Ushio, D. Yokomizo, T. Kanadani: *Mater. Trans.*, 2013, **54**, 199–206.
37. F.C. Walsh, C.P. de Leon, C. Kerr, S. Court, B.D. Barker: *Surf. Coat. Technol.*, 2008, **202**, (21), 5092–5102.
38. S. Court, C. Kerr, C. Ponce de Leon, J.R. Smith, B.D. Barker, F.C. Walsh: The influence of iodate ion additions to the bath on the deposition of electroless nickel on mild steel, *Trans. IMF*, 2017, to be submitted.

Table captions

Table 1. Induction times for electroless Ni plating in a Fidelity 5010 bath, a Fidelity 4355 bath and a proprietary bath at 90 °C following a single or double zincating pre-treatment at 22 °C.

Table 2. Open-circuit electrode potentials at which electroless Ni plating initiated in proprietary baths at 90 °C, following a single or double zincating pre-treatment at 22 °C.

Figure captions

Fig. 1. The experimental arrangement used to monitor the induction time of electroless Ni coatings.

Fig. 2. Potential vs. time curve for the deposition of electroless Ni on Al at 22 °C from which the induction time for electroless Ni plating can be calculated. The potentials of pure Ni, Zn and untreated Al are shown for comparison.

Fig. 3. Potential vs. time curves in Fidelity 5010 electroless Ni at 90 °C for Al following a: (a) single zincate in 20% Fidelity 3116M zincate solution, (b) double zincate in 20% Fidelity 3116M zincate solution, (c) single zincate in 40% Fidelity 3116M zincate solution, and (d) single zincate in the Laboratory prepared, concentrated zincate solution; all at 22 °C.

Fig. 4. (a) Current vs. time and (b) potential vs. time curves during one hour immersion in a Fidelity 4355 electroless Ni bath at 90 °C for Al treated by a double zincate in 40% vol. Fidelity 3116M zincate solution at 22 °C.

Fig. 5. Coating thickness vs. immersion time in: 20% vol. zincate solution, 40% vol. zincate solution, laboratory prepared dilute (LD) zincating solution, and laboratory prepared concentrated (LC) zincate solution; all at 22 °C, also showing differences between

single and double zincating pre-treatment (suffix 'S' and 'D' after 20, 40, LD and LC immersions).

Fig. 6. SEM images of Al surfaces after a (a) single zincate pretreatment procedure of 60 s, and (b) double zincate pretreatment procedure each of 60 s; magnifications 500 \times . Inset images show increased magnifications of 2500 \times . All scale bars represent 10 μm .

Fig. 7. AFM micrographs of Al surfaces after zincate pre-treatments: (a,b) a single zincate pre-treatment (10 $\mu\text{m} \times 10 \mu\text{m}$ and 5 $\mu\text{m} \times 5 \mu\text{m}$, respectively), and (c,d) a double zincate pre-treatment (10 $\mu\text{m} \times 10 \mu\text{m}$ and 5 $\mu\text{m} \times 5 \mu\text{m}$, respectively).

Fig. 8. Schematic cross-section of the surface layers on an Al alloy substrate following various zincate pre-treatments: (a) single zincate in synthetic laboratory solution, (b) double zincate in synthetic laboratory solution, (c) single zincate in proprietary solution, and (d) double zincate in a proprietary solution.

Table 1

Electroless Ni deposit induction time, t_i / s													
Single zincating immersion time, t / s	Double zincating immersion time, t / s	Synthetic		Fidelity		Synthetic		Fidelity 5110		Synthetic		Proprietary	
		Laboratory	bath	3116M	Bath	Laboratory	bath	zincating	zincating	Laboratory	bath	zincating	solution
		Dil	Conc	20%	40%	Dil	Conc	20%	40%	Dil	Conc	20%	40%
120	0	24.1	28.8	36.0	27.2	28.2	20.8	47.2	44.8	24.0	28.8	36.3	27.2
90	0	21.6	26.4	35.2	28.4	22.4	20.1	41.6	42.4	21.6	26.4	35.2	28.0
60	0	20.2	24.0	34.4	27.2	22.4	19.2	32.8	43.2	20.0	24.0	34.4	27.2
30	0	16.0	19.2	32.2	22.4	18.4	16.3	26.4	35.2	16.1	19.2	32.1	22.4
15	0	12.2	14.4	28.1	21.6	14.4	14.4	23.2	32.1	12.1	14.4	28.0	21.6
60	120	12.3	15.2	22.4	28.8	18.4	15.2	27.2	29.6	12.1	15.2	22.4	28.8
60	90	11.2	14.4	20.8	29.6	17.6	16.4	24.8	24.8	11.2	14.4	20.8	29.6
60	60	11.2	14.4	20.1	23.2	16.8	15.2	25.6	25.6	11.2	14.4	20.2	23.2
60	30	9.6	13.6	16.8	19.2	14.4	13.6	24.0	24.0	9.6	13.6	16.8	19.2
60	15	8.1	11.2	16.0	17.6	13.6	10.4	21.6	19.2	8.2	11.2	16.1	17.6

Table 2

Zincating solution	Open-circuit potential for initiation of electroless Ni deposition, E vs. SCE / V			
	Fidelity 5010 bath		Fidelity 4355 bath	
	Single	Double	Single	Double
Dilute Synthetic laboratory	-0.655	-0.652	-0.633	-0.629
Concentrated Synthetic laboratory	-0.650	-0.650	-0.634	-0.631
20% Fidelity 3116M	-0.668	-0.666	-0.642	-0.642
40% Fidelity 3116M	-0.668	-0.668	-0.638	-0.641

Figures

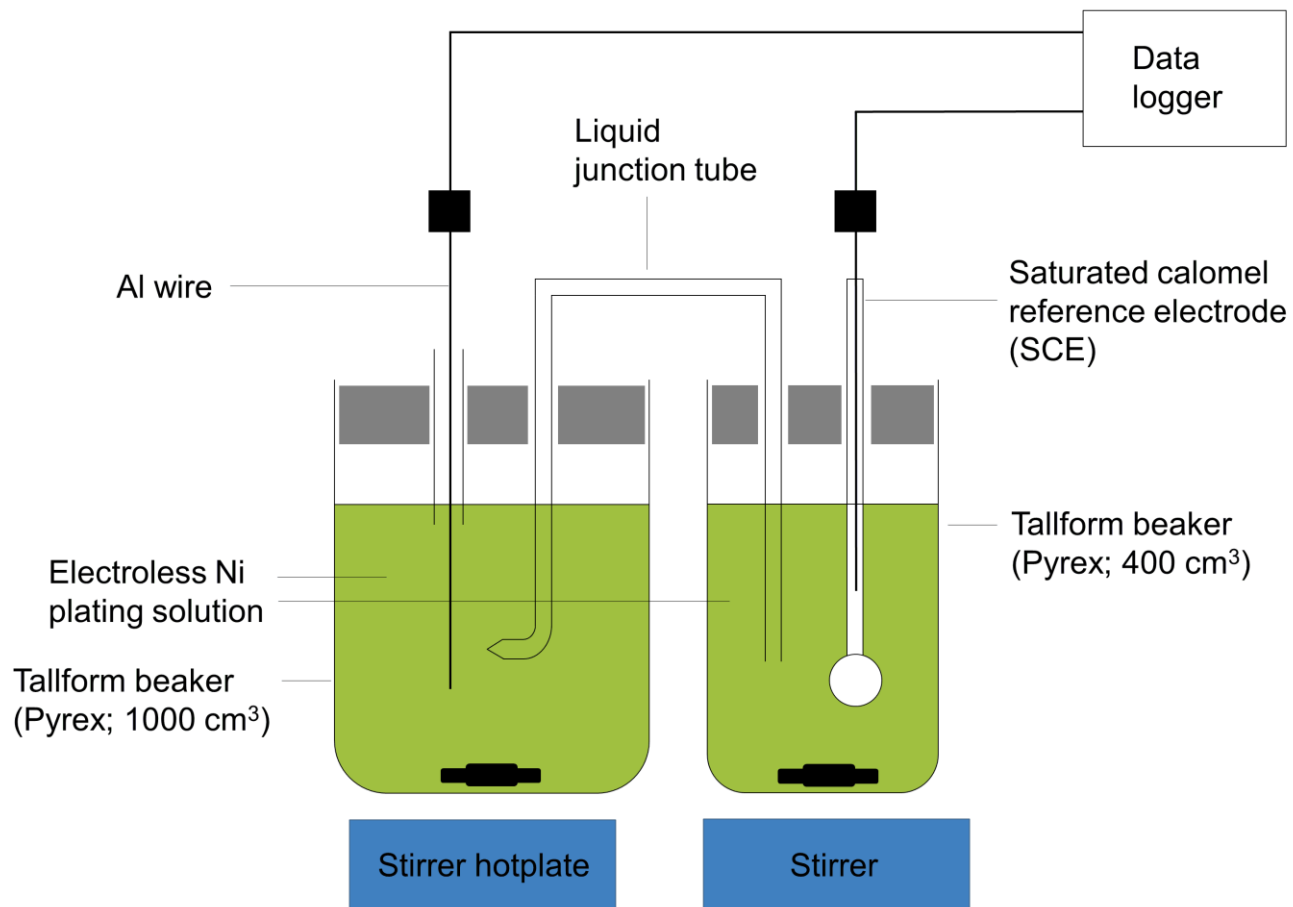


Fig. 1

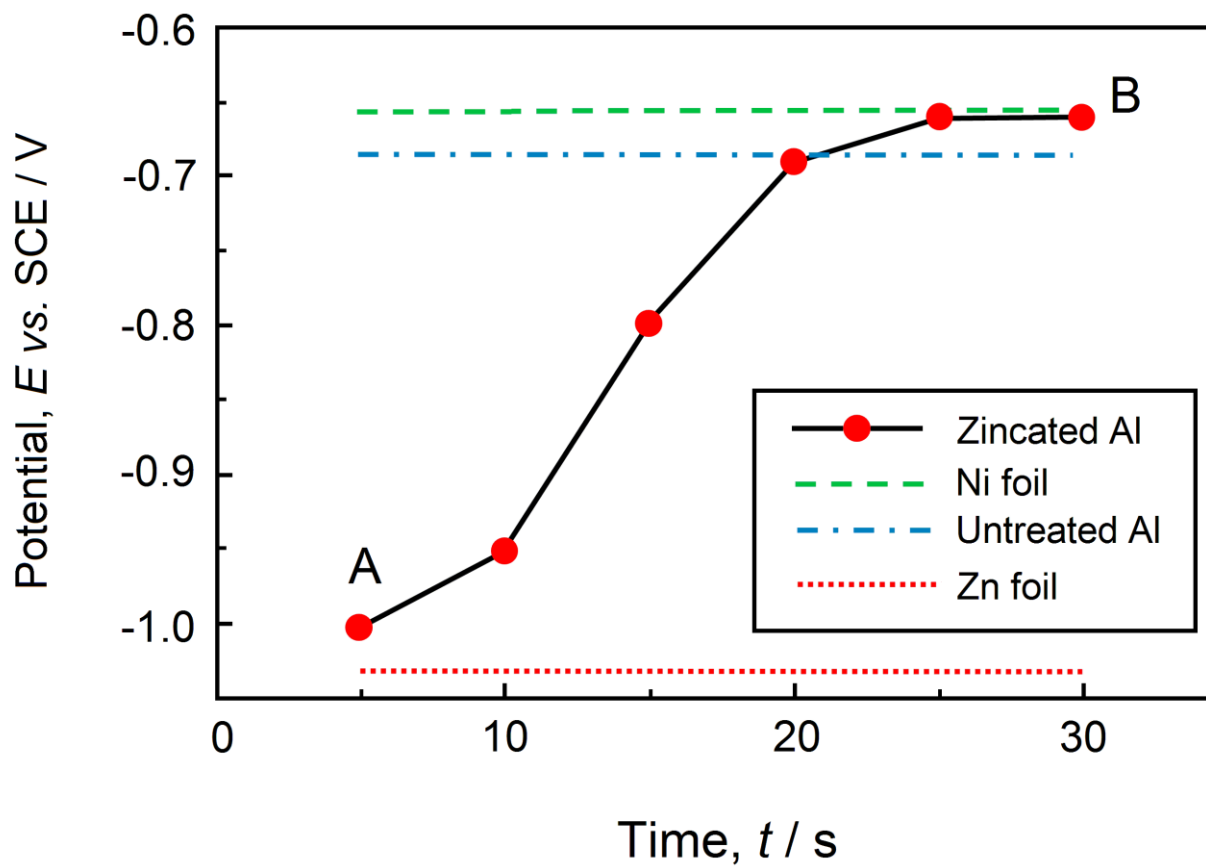


Fig. 2

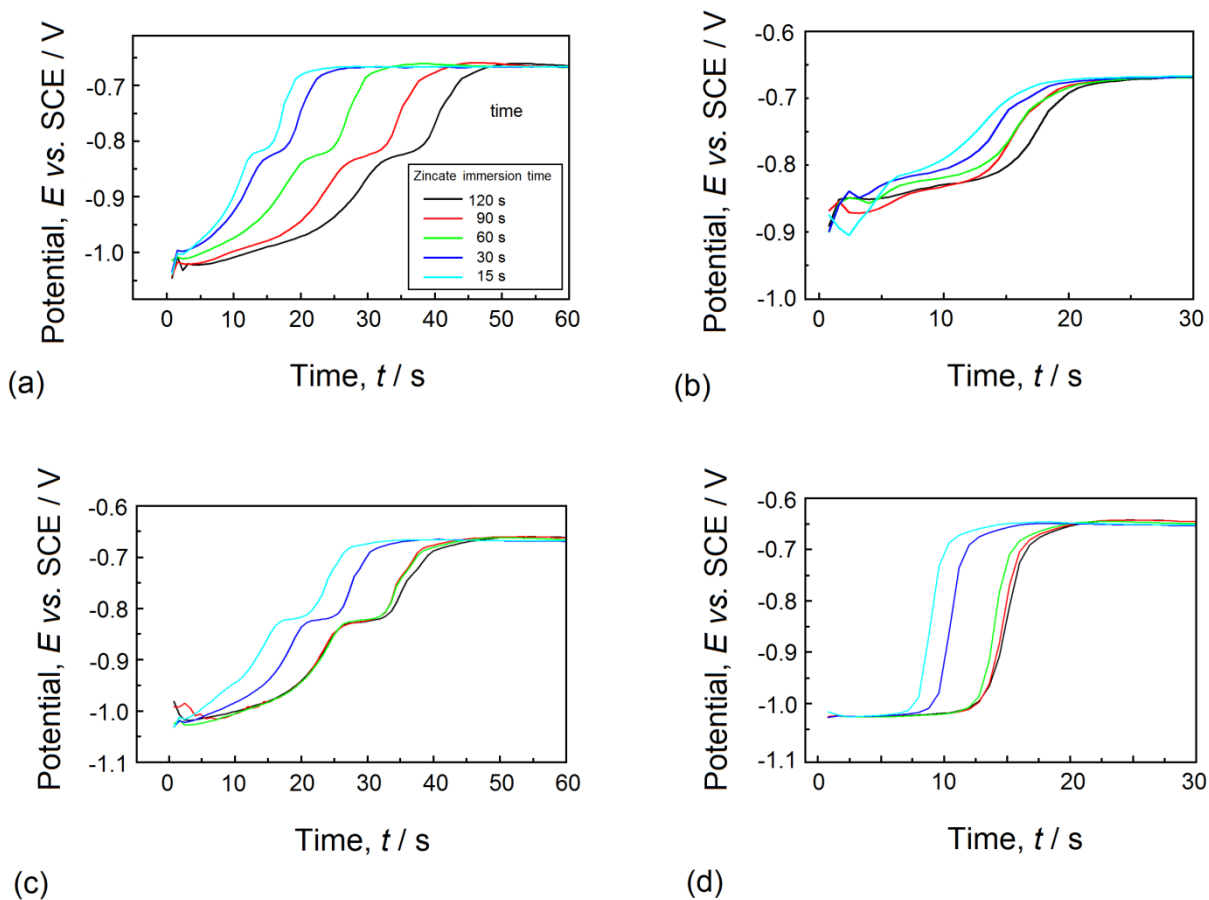


Fig. 3

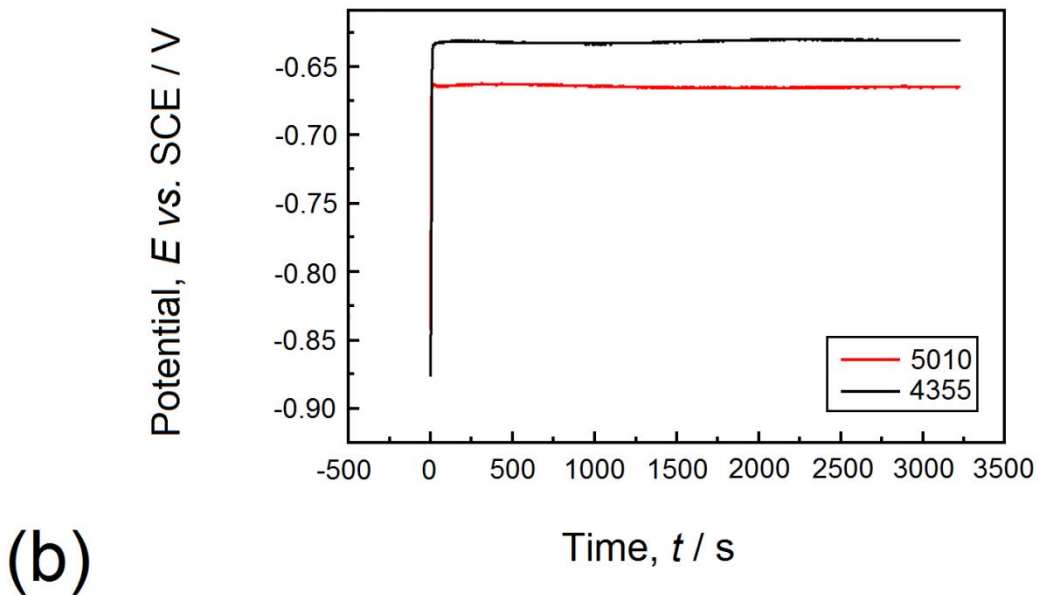
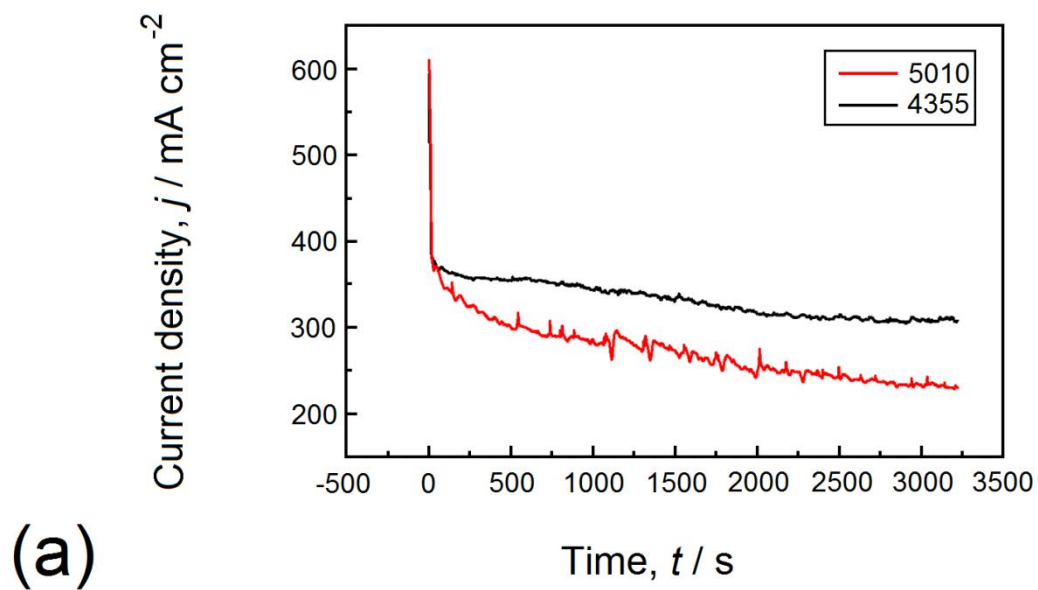


Fig. 4

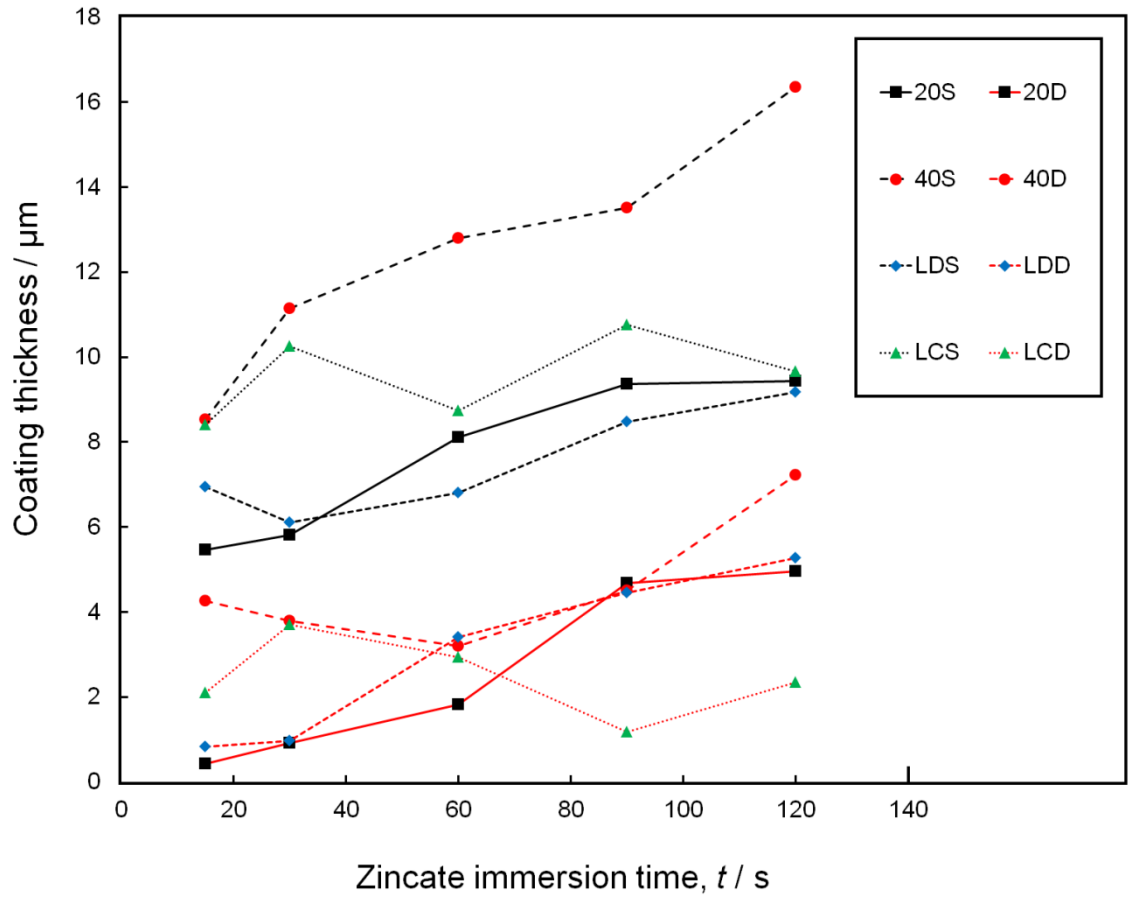


Fig. 5

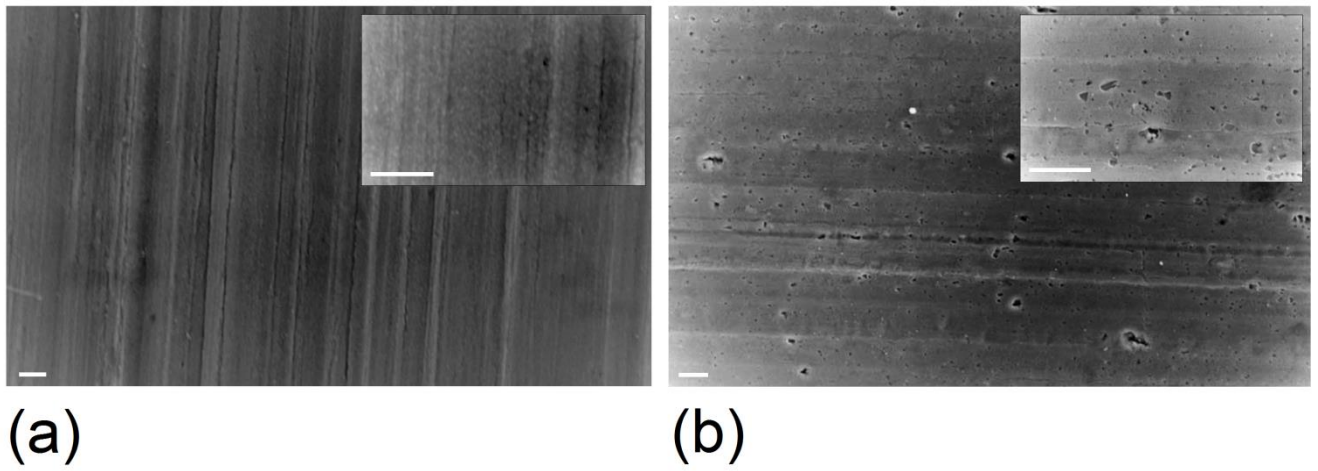


Fig. 6

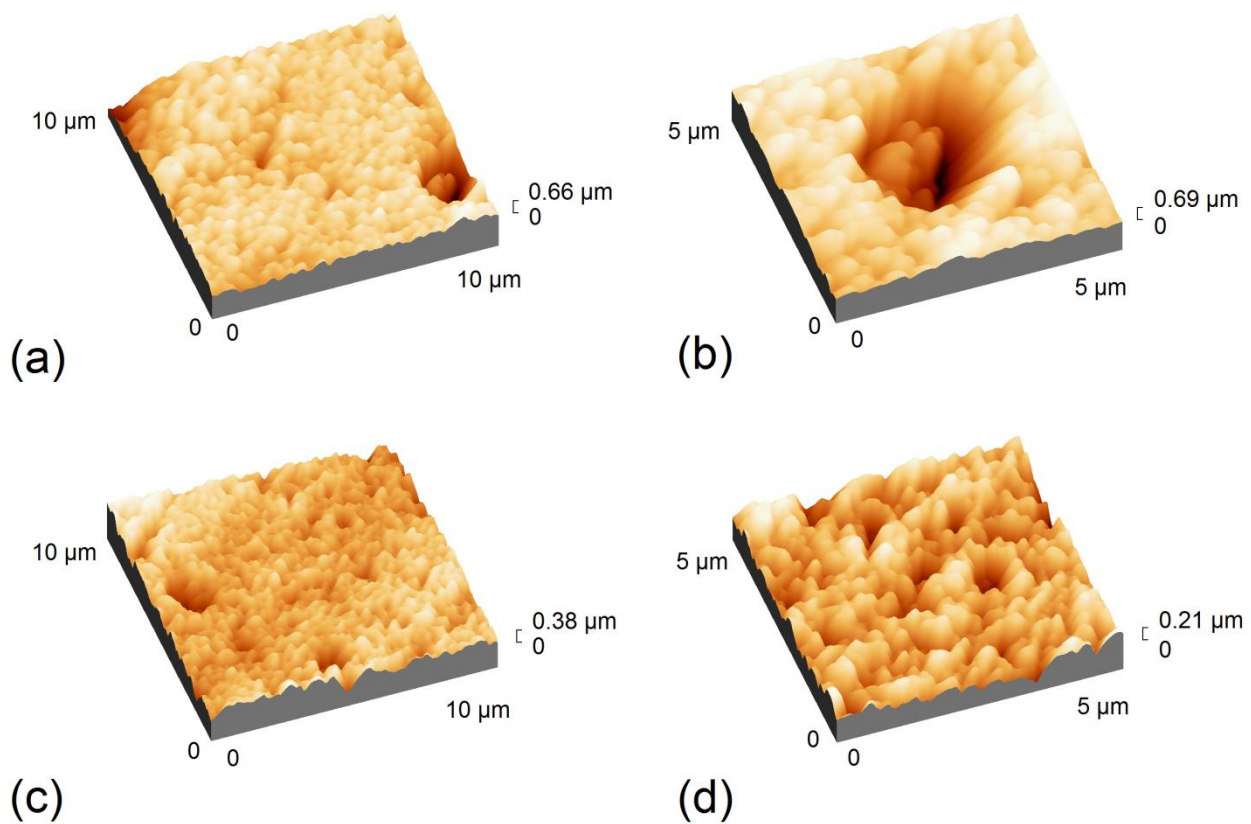


Fig. 7

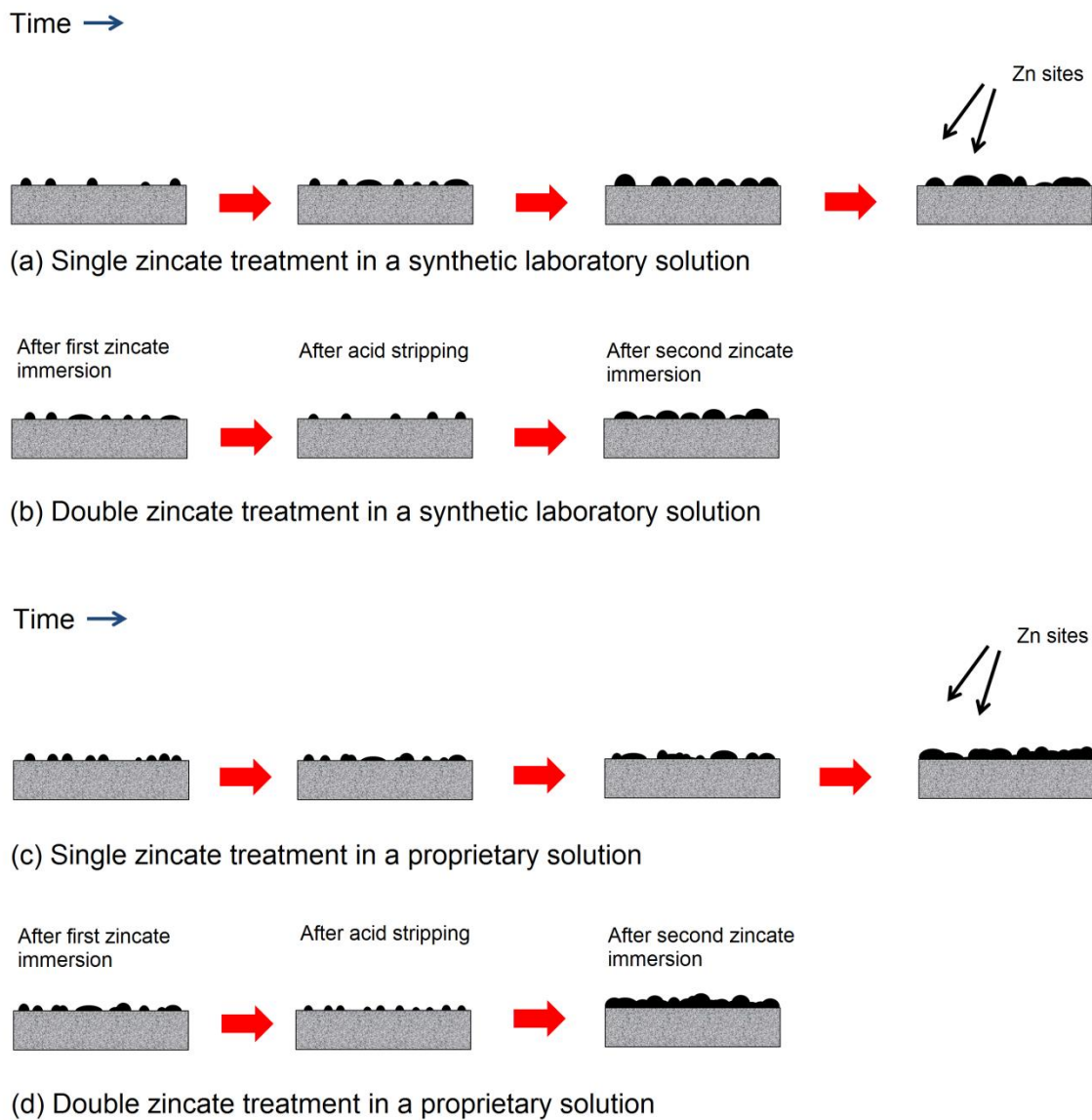


Fig. 8